# MODELLING THE START-UP FLOW OF WELL DRILLING FLUIDS

**Leandro Lourenço Vieira da Rocha, leandrolvrocha@gmail.com**
**Gabriel Mehry de Oliveira, gabrielmerhy@hotmail.com**
**Cezar Otaviano Ribeiro Negrão, negrao@utfpr.edu.br**
**Admilson Teixeira Franco, admilson@utfpr.edu.br**
Universidade Tecnológica Federal do Paraná, Depart. Acadêmico de Mecânica, Laboratório de Ciências Térmicas
Avenida Sete de Setembro, 3165 – 80230-901 – Rebouças – Curitiba – Paraná – Brazil

**André Leibsohn Martins, aleibsohn@petrobras.com.br**
TEP / CENPES / PETROBRAS
Avenida Jequitibá, Block 7 – 21941-598 – Ilha do Fundão – Rio de Janeiro – Rio de Janeiro – Brazil

***Abstract.*** *Many oil well drilling fluids are designed to gel when it is not submitted to shear stress. The purpose is to avoid cuttings to lie over the bit during the circulation stoppage. When circulation resumes the pumping pressure rises above the circulation pressure in order to overcome the gel strength. Due to its thyxotropic effect, the gel viscosity remains high for a while after the circulation restarts. The gelation may have significant importance, specially, in deep waters where high pressures and low temperatures take place. The current work presents a compressible transient flow model of the start-up flow of drilling fluids, in order to predict borehole pressures. The model comprises the one-dimensional conservation equations of mass and momentum. A second order differential equation is derived from the sum of the governing equations. This equation is one variable dependent, the velocity, and it is easier to solve. it is discretized by the Finite Volume Method and solved. The pressure is obtained after the whole velocity field for each time-step is found. This alternative solution is compared to the simultaneous solution of the conservation equations of mass and momentum. The viscous effect is modeled by employing the friction factor approach. The Fanning friction factor for Bingham fluid is changed in order to avoid indetermination when velocity tends to zero and a fourth order solution is proposed for the friction factor. The results are corroborated with the literature. A sensibility analysis with respect to Reynolds number, Bingham number and compressibility was also carried out.*

***Keywords****: drilling fluid, transient flow, Bingham's friction factor*

## 1. INTRODUCTION

Well drilling is not a continuous operation and interruptions for maintenance are quite common. The drilling fluid builds up a gel-like structure when the flow stops, in order to avoid the cuttings to lie over the drill bit and therefore to obstruct and damage it. On the other hand, pump pressures higher than the continuous operation pressure are needed to break the gel.

Several works have developed models for the start-up of fluid flows. Sestak *et al*. (1987), for example, has discussed an approach to predict the time to clear out a pipeline full of gelled crude oils. The clearing Newtonian fluid was modeled as incompressible and the gelled fluid as compressible non-Newtonian. The time dependent rheology properties were described by Houska´s thyxotropy model (apud Sestak *et al.*, 1987), which is a generalization of Bingham and Power Law fluid models. Escudier (1996) investigated some fluids with thixotropic characteristics and emphasized the importance of the studies about this kind of flow. The author says the Herschel-Bulkley model describes quite well the laminar and turbulent flows of a thyxotropic fluid. However, instabilities were observed in the flow transition.

Chang *et al.* (1998) conducted experimental tests to evaluate the Wardhaugh and Boger´s (1991) theory for thyxotropic fluids under shear stress. This theory divides the fluid stress response into three: elastic response, creep and fracture. Engineers are mostly interested in the static yield stress (the stress value when the fracture occurs) as this stress value effectively determines the pump capacity required to initiate the flow.

In their later work, Chang *et al.* (1999) developed a mathematical model for an isothermal start-up flow of a waxy crude oil. The model was based on the three yield stresses response described in the previous work. The time response of the flow rate and the clean-up time of an incompressible gel were evaluated. The inlet pressure was considered a constant value and the Bingham fluid model was employed.

Vinay *et al.* (2006 and 2007) compared a two-dimensional with a one-dimensional mathematical model for the gelled fluid flow in axisymmetric pipes. They showed the results are very similar. However, the calculations for the two-dimensional model are quite slow in comparison to the one-dimensional ones.

The current work presents a model for the start-up of drilling fluids in a horizontal pipe. The transient fluid flow is considered one-dimensional and compressible. The non-linear differential equations are discretized and solved by the Finite Volume Method and the non-Newtonian drilling fluid is considered as a Bingham fluid.

## 2. MATHEMATICAL MODELING

The transient flow of the Bingham fluid is modeled as one-dimensional and compressible in a horizontal pipe. The viscosity and the fluid compressibility are considered constant. The Fanning friction factor is employed to take into account the wall shear stress. The behavior of the Bingham fluid can be described as:

$$\begin{aligned} &\tau = \tau_0 + \mu_p \dot{\gamma} && \tau > \tau_0 \\ &\dot{\gamma} = 0 && \tau \le \tau_0 \end{aligned} \tag{1}$$

where $\tau$ is the shear stress, $\tau_0$ is the yield stress, $\mu_p$ is the plastic viscosity and $\dot{\gamma}$ is the shear strain rate. According to Eq. (1), the fluid flows only if the shear stress is greater than the yield stress. In a pipeline, the flow of a Bingham fluid presents a uniform velocity plug because of the yield stress: a central core in which no shearing takes place (see Fig. 1).

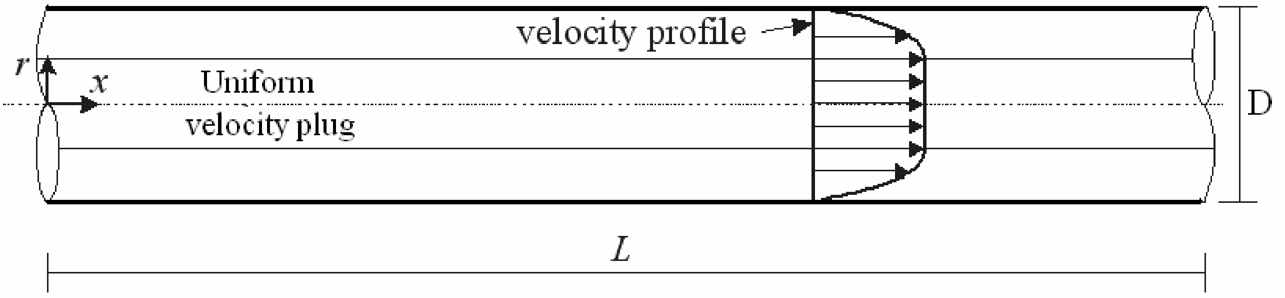


Figure 1 – Representation of the developed velocity profile in a pipe for a Bingham fluid.

The problem domain consists of a pipe with diameter $D$ and length $L$. The flow is described by the conservation equation of mass:

$$\frac{\partial u}{\partial x} + \alpha \frac{\partial P}{\partial t} = 0 \tag{2}$$

and momentum:

$$\rho \frac{\partial u}{\partial t} + \frac{\partial P}{\partial x} + \frac{2\rho f}{D} u^2 = 0 \tag{3}$$

where $u = u(x,t)$ is the flow velocity, $P = P(x,t)$ is the pressure, $\alpha$ is the fluid compressibility, $\rho$ is the fluid density and $f$ is the Fanning friction factor, defined as $f = \frac{\tau_w}{½ \rho u^2}$. $\tau_w$ is the shear stress on the pipe wall.

One can see the axial change of density and velocity, respectively, in the conservation equation of mass and momentum are disregarded. Although these hypotheses were also adopted by Cawkwell and Charles (1987) these effects will be evaluated in a future work.

The friction factor for the laminar flow of a Bingham fluid can be computed as:

$$f = \frac{16}{\mathrm{Re}} \left( 1 + \frac{\mathrm{He}}{6\,\mathrm{Re}} - \frac{\mathrm{He}^4}{3 f^3 \,\mathrm{Re}^7} \right) \tag{4}$$

where $\mathrm{Re} = \rho u D / \mu_p$ is the Reynolds number and $\mathrm{He} = \tau_0 \rho D^2 / \mu_p^2$ is the Hedstrom number.

Initially, the fluid stands still within the pipe and therefore the initial conditions are described as:

$$u(x,0) = 0 \tag{5}$$

$$P(x,0) = 0 \tag{6}$$

A pressure pulse is thus imposed at the pipe inlet:

$$P(0,t) = P_B us(t) = \begin{cases} us(t) = 0 & t = 0 \\ us(t) = 1 & t > 0 \end{cases} \tag{7}$$

where $P_B$ is a constant pressure value and $us(t)$ is a step function. At the outlet, the pressure is kept equal to zero:

$$P_s = 0 \quad \forall t \tag{8}$$

Note that Eqs. (2) and (3) must be solved simultaneously in order to obtain the solution for both velocity and pressure. A mathematical manipulation is carried out in order to simply the solution. First of all, Eq. (2) is differentiated with respect to x and Eq. (3) with respect to t. The resulting equations are subtracted from each other and the following equation is found:

$$\rho \frac{\partial^2 u}{\partial t^2} - \frac{1}{\alpha} \frac{\partial^2 u}{\partial x^2} + \frac{2\rho}{D} \frac{\partial \left( f u^2 \right)}{\partial t} = 0 \tag{9}$$

As can be seen, Eq. (9) depends only on the velocity and is solved independently on the pressure. Once velocity is known it can be substituted either in Eq. (2) or (3) in order to obtain the pressure. However, the non-linear Eq. (9) requires an iterative solution, which is discussed in section 2.2. Two initial and two boundary conditions are needed in Eq. (9). As the fluid is stagnant at the start-up, the velocity field (Eq. (4)) and its time change ( $\partial u / \partial x|_{t=0} = 0$ ) are considered null. According to Eq. (7) and (8), the pressures are known at both boundary but not the velocity. To find the velocity boundary conditions, Eq. (2) is applied at the inlet and outlet:

$$\left. \frac{\partial u}{\partial x} \right|_{x=0} = -\alpha \left. \frac{\partial P}{\partial t} \right|_{x=0} = -\alpha \delta(t) P_B \tag{10}$$

$$\left. \frac{\partial u}{\partial x} \right|_{x=L} = \alpha \left. \frac{\partial P}{\partial t} \right|_{x=L} = 0 \tag{11}$$

where $\delta(t)$ is the Dirac Delta function, also called as Unit Impulse function, which is the result of the differentiation of function $\mathrm{us}(t)$.

### 2.1. The Friction Factor's Equation

Once Eq. (4) is a non-linear implicit equation the friction factor must be obtained iteratively. However, if Eq. (4) is written as,

$$f^4 - f^3 \left( \frac{16}{\mathrm{Re}} + \frac{8\mathrm{He}}{3\mathrm{Re}^2} \right) + \frac{16\mathrm{He}^4}{3\mathrm{Re}^8} = 0 \tag{12}$$

a solution can be found for the fourth order equation. Two of the four roots of Eq. (11) are complex and only one of the real ones is physically possible. To find out which is the feasible one, the definition of uniform velocity plug radius is used. Actually, only one of the roots presents a uniform velocity plug plug radius smaller than the pipe radius. This is accomplished by satisfying the following condition:

$$\frac{f\ \mathrm{He}}{\mathrm{Re}^2} \leq 1 \tag{13}$$

As the velocity field starts from the rest, the Reynolds number approaches to zero and therefore the friction factor tends to infinity (see Figure 2a). This singularity must be solved otherwise Eq. (9) cannot be solved. Note, however, that the product $f\,\mathrm{Re}^2$ comes close to a constant value as the Reynolds number goes to zero (see Fig. 2b). This constant value depends only on the Hedstrom number. The product $f\,\mathrm{Re}^2$ can be directly substituted in Eq. (9) as the friction term depends on the product of friction factor and velocity square. Hence, Eq. (12) is modified and written as:

$$\left[f\,\mathrm{Re}^2\right]^4 - \left[f\,\mathrm{Re}^2\right]^3\left(16\,\mathrm{Re} + \frac{8\mathrm{He}}{3}\right) + \frac{16\mathrm{He}^4}{3} = 0 \tag{14}$$

Equation (14) has two known real roots which are shown in Rocha (2007).

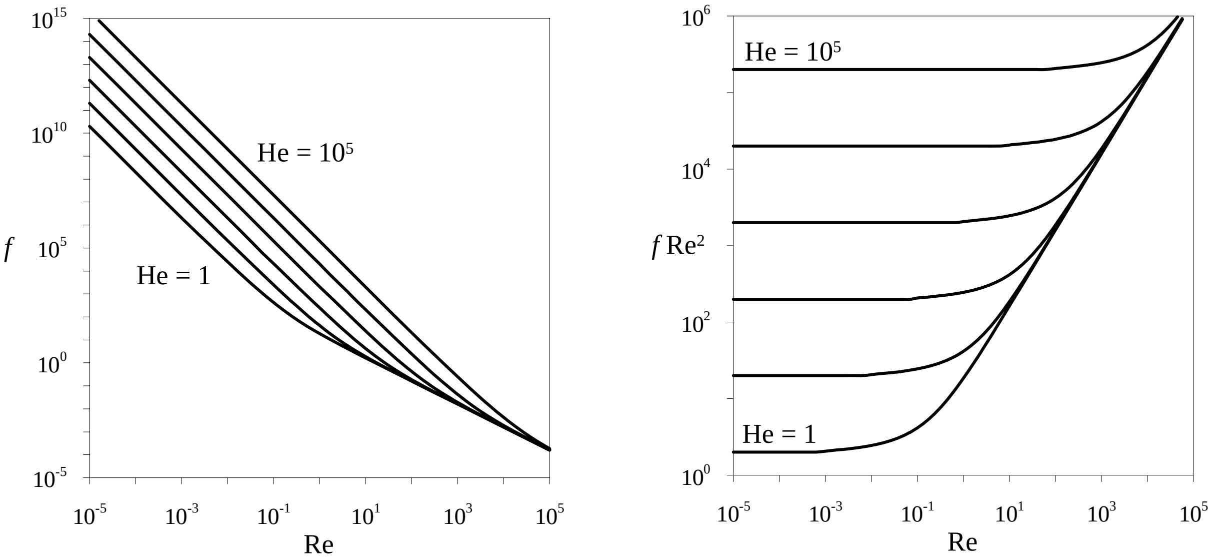


(a) f x Re

(b) f $\mathrm{Re}^2$ x Re

Figure 2 – (a) $f$ and (b) $f \cdot \mathrm{Re}^2$ as a function of Re for various He.

## 2.2. The Solution Algorithm

As already mentioned, the governing Eq. (9) is a non-linear partial differential equation and therefore requires an iterative numerical solution. Besides, this equation is hyperbolic and one of its boundary condition is a discontinuous function (Eq. (10)). Because of the hyperbolic characteristic of the equation the time and space grid sizes have to satisfy the Courant-Friedrichs-Lewy (CFL) stability criterion (Fortuna, 2000). The CFL criterion establishes that the ratio of space and time grid sizes must be smaller than or equal to the pressure wave speed. The velocity and pressure grids are staggered. Different from the usual staggered grids, the pressures are placed at the boundary of the domain. Both space and time grids are uniform.

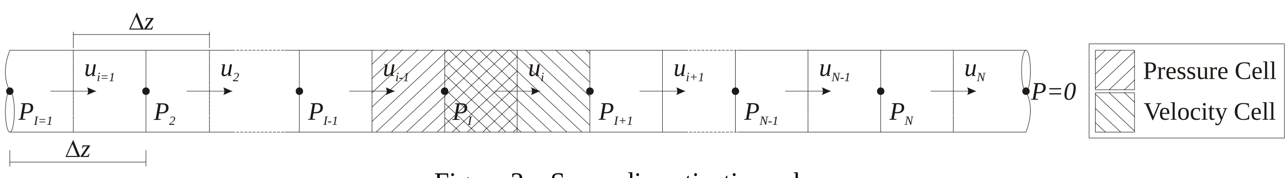


Figure 3 – Space discretization scheme

Equation (9) is discretized by the Finite Volume Method and a set of algebraic equations is obtained:

$$A_i u_i^{n+1} + B_i u_{i+1}^{n+1} + C_i u_{i-1}^{n+1} = D_i \tag{15}$$

where the index $i$ corresponds to the $i^{th}$ velocity position and $n+1$ corresponds to the future time step. The coefficients are defined for each point of the domain, as follows:

$$A_i = \begin{cases} \dfrac{\rho\Delta x}{\Delta t} + \dfrac{2\Delta t}{\alpha\Delta x} & 2 \le i < N \\ \dfrac{\rho\Delta x}{\Delta t} + \dfrac{\Delta t}{\alpha\Delta x} & i = 1 \text{ ou } i = N \end{cases} \tag{16}$$

$$B_i = \begin{cases} -\dfrac{\Delta t}{\alpha\Delta x} & i < N \\ 0 & i = N \end{cases} \tag{17}$$

$$C_i = \begin{cases} 0 & i = 1 \\ -\dfrac{\Delta t}{\alpha\Delta x} & i > 1 \end{cases} \tag{18}$$

$$D_i = \begin{cases} 2\rho\Delta x\left[\dfrac{1}{\Delta t} + \dfrac{\left(fu^2\right)_i^n - \left(fu^2\right)_i^{n+1}}{D} - \dfrac{1}{2\Delta t}u_i^{n-1}\right] & \begin{matrix} i > 1 \text{ ou} \\ i = 1 \text{ e } n > 1 \end{matrix} \\ P_B - \dfrac{2\rho\Delta x}{D}\left(fu^2\right)_i^{n+1} & i = 1 \text{ e } n = 1 \end{cases} \tag{19}$$

where $\Delta x$ is the space grid size, $\Delta t$ is the temporal increment and $N$ is the number of finite volumes.

Equation (2) is also discretized by Finite Volume Method in order to compute the pressure field at each time-step:

$$P_{I+1}^{n+1} = P_I^{n+1} - \frac{\Delta t}{\alpha\Delta z}\left(u_i^{n+1} - u_i^n\right) \tag{20}$$

The set of Eq. (15) is solved by TDMA Algorithm (Three-Diagonal Matrix Algorithm). However, the coefficient $D_i$ (Eq. (19))* depends on the velocity field being calculated and therefore, an iterative solution is employed each time-step. The solution algorithm follows the steps below:

1. Initialization: $P_B$, $L$, $D$, $\rho$, $\mu$, $\alpha$, $\tau_{yo}$, $\tau_{y\infty}$, $\kappa$, $N$ (or $\Delta x$) $\Delta t$, $u(x,t=0)=0$ and $\dfrac{\partial u}{\partial t}(x,t=0)=0$.
2. Estimation of the initial velocity field ($u_i^{n+1}$) for $n = 0$ and calculation of $\left(fu^2\right)_i^{n+1}$.
3. Calculation of the coefficients $A_i$, $B_i$, $C_i$ and $D_i$ and the solution of Eq. (15) by TDMA to obtain $u_i^{n+1}$.
4. If the difference between the velocity field in two consequent iterations is greater than a convergence criterion ($\varepsilon$), return to step 2 otherwise go to step 5.
5. Calculation of $P_I^{n+1}$ (Eq. (20)) based on the values of $u_i^{n+1}$.
6. In case the flow has achieved the steady state, the algorithm is stopped, otherwise return to step 2 for the next time-step ($n = n+1$).

## 3. RESULTS AND DISCUSSION

In order to compare the current model with the literature data, the results are normalized according to Vinay *et al*. (2007). Three parameters for the Bingham fluid flow in a pipe are defined: the Reynolds number ($\mathrm{Re}^*$), the Bingham number ($\mathrm{B}^*$) and a dimensionless compressibility ($\alpha^*$):

$$\mathrm{Re}^* = \frac{\rho P_B D^4}{16\mu_p^2 L^2} \tag{21}$$

$$B^* = \frac{2\tau_0 L}{P_B D} \tag{22}$$

* Note that the ratio of $fu^2$ and $f\,\mathrm{Re}^2$ is the constant $\left(\mu/\rho D\right)^2$

$$\alpha^* = \alpha P_B \tag{23}$$

The dimensionless axial coordinate and pressure are, respectively, $x^* = x / L$ and $P^* = P / P_B$. The dimensionless velocity and time are defined, respectively, as:

$$u^* = u \frac{4\mu L}{P_B D^2} \tag{24}$$

$$t^* = t \frac{u^*}{\alpha^* L} \tag{25}$$

Figure 4 shows a comparison of current model results with the Vinay´s *et al.* (2007) data for $\mathrm{Re}^* = 0.001$, $\mathrm{B}^* = 0.1$ and $\alpha^* = 0.1$. One can see the results are quite similar for this compressibility. However, for higher compressibility, discrepancies between the models are noted. The inlet and outlet velocities are compared in Figure 5 for $\mathrm{Re}^* = 0.001$, $\mathrm{B}^* = 0.1$ and $\alpha^* = 1.0$. Note that the steady inlet and outlet velocities of the current model coincide to each other. On the other hand the Vinay´s counterpart values are quite different from each other as the flow accelerates from the inlet to the outlet. As the axial density changes are disregarded in the continuity equation, the current model results do not show such acceleration. Therefore, the current model is adequate for low but not high compressibility.

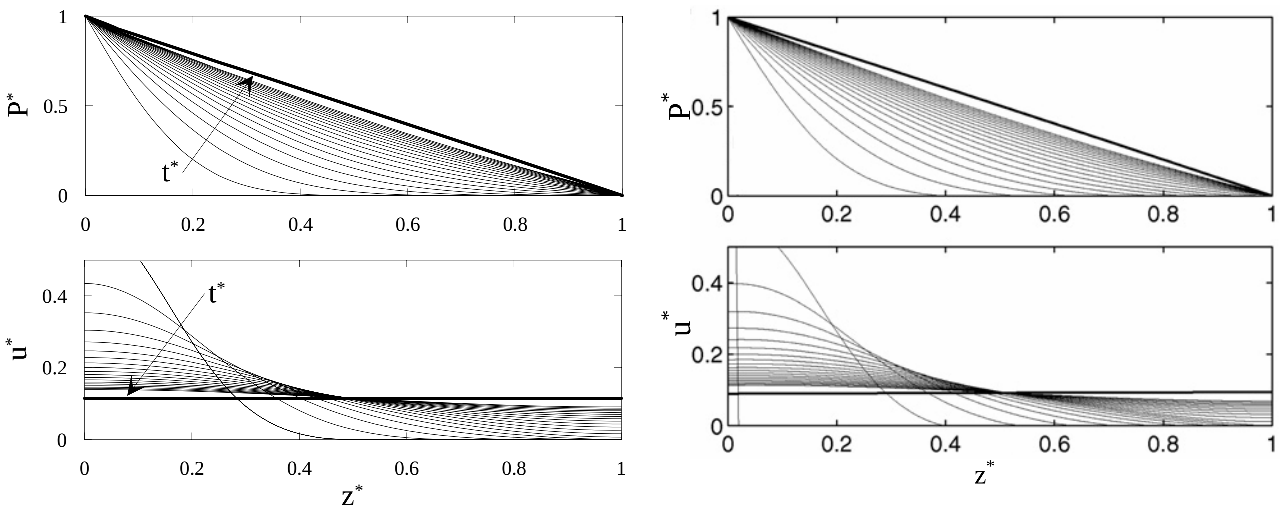


(a) (b)

Figure 4 – Dimensionless velocity and pressure fields ($t^*$ = 0.1, 0.2, ..., 2.0) for $\mathrm{Re}^* = 0.001$, $\mathrm{B}^* = 0.1$ and $\alpha^* = 0.1$ (a) current model and (b) obtained from VINAY *et al.* (2007)

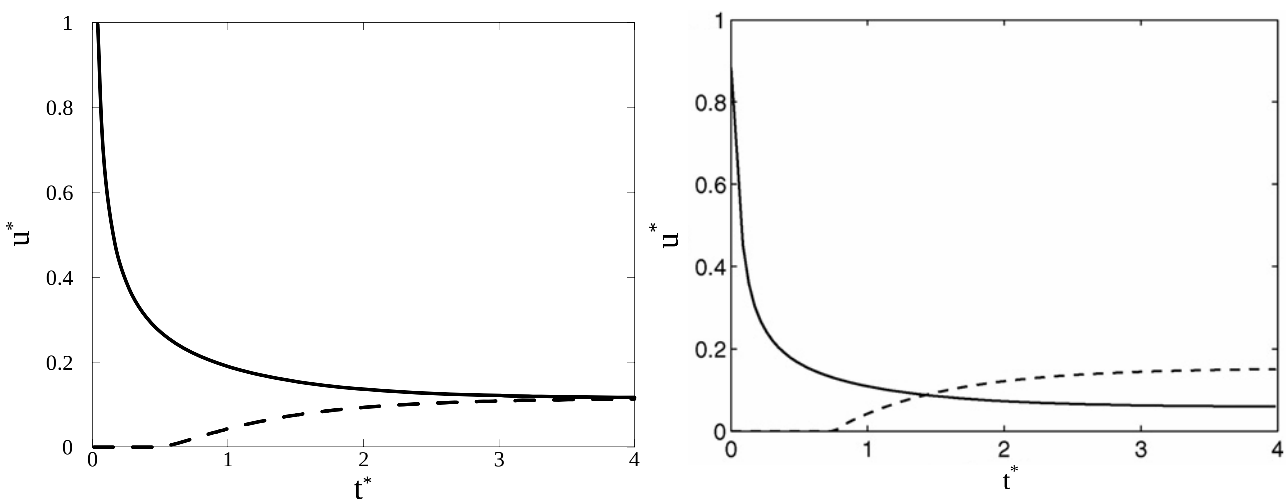


(a) (b)

Figure 5 – Time change of the inlet and outlet (dashed line) velocities for $\mathrm{Re}^* = 0.001$, $\mathrm{B}^* = 0.1$ and $\alpha^* = 1.0$ .
(a) Current model and (b) obtained from VINAY *et al.* (2007)

A sensitivity analysis is now conducted. Figure 6 shows the sensitivity of the pressure at the position z*=0.9 with respect to the Reynolds number, the Bingham number and to the dimensionless compressibility. As can be seen, the pressure oscillates in a high frequency for low compressibility values and the first peak reaches almost 60% of the inlet pressure for Re*=0.4. These oscillations are caused by the reflection of the pressure wave at the pipe outlet and inlet, because the pressures are fixed at those positions. As the viscous effect dampens the pressure propagation, the reduction of the Reynolds number diminishes the amplitude of the pressure peaks maintaining the oscillation frequency. The increase of the compressibility also softens the pressure amplitude and reduces the time needed for steady state to be reached (Compare Figures 6a and 6b). Although the increase of Bingham slightly reduces the pressure peaks the oscillation frequency does not change.

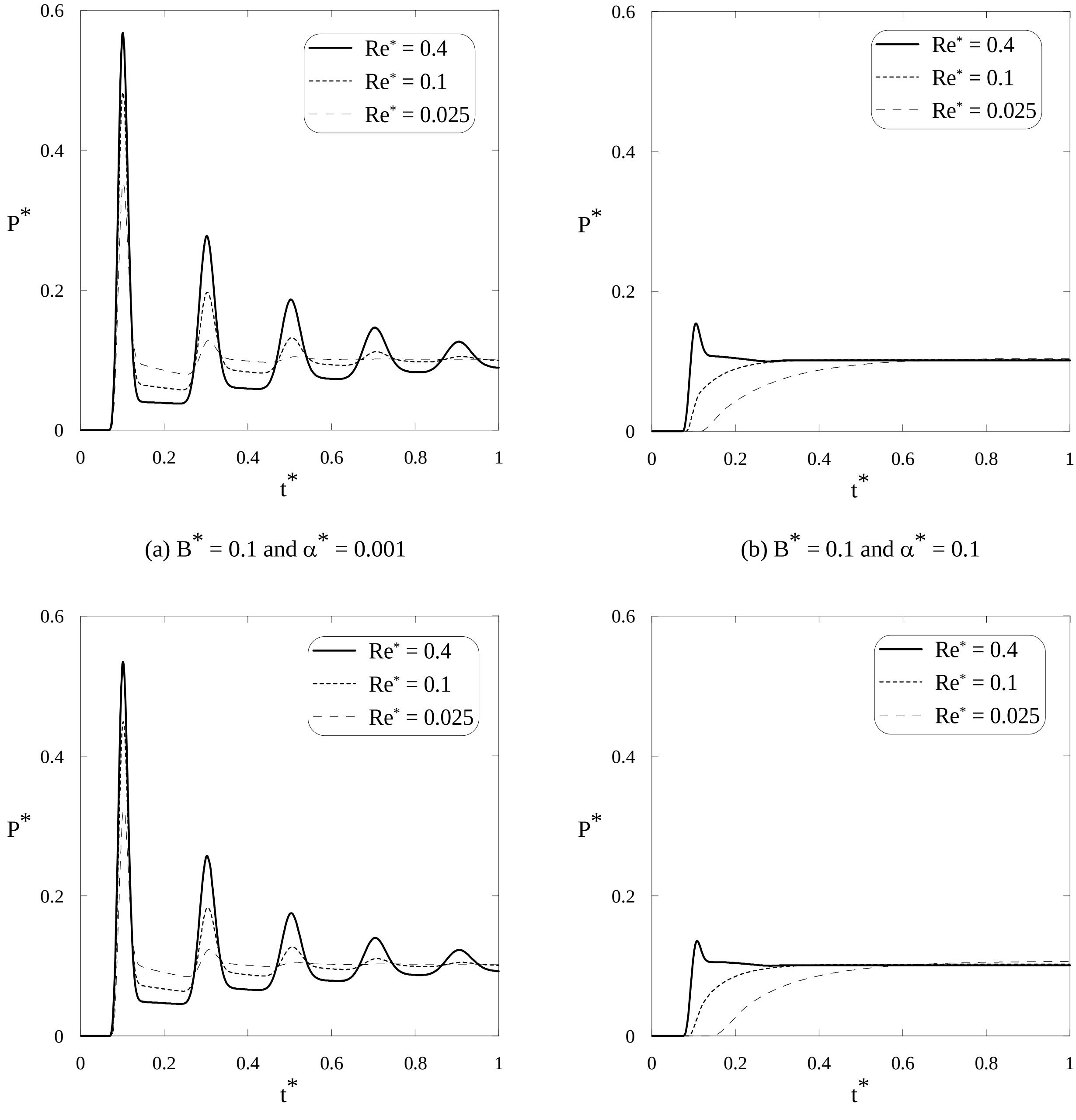


(a) $\mathrm{B}^* = 0.1$ and $\alpha^* = 0.001$

(b) $\mathrm{B}^* = 0.1$ and $\alpha^* = 0.1$

(c) $\mathrm{B}^* = 0.4$ and $\alpha^* = 0.001$

(d) $\mathrm{B}^* = 0.4$ and $\alpha^* = 0.1$

Figure 6 – Pressure temporal variation in $z^* = 0.9$ for different values of $\mathrm{Re}^*$, $\mathrm{B}^*$ and $\alpha^*$.

## 4. CONCLUSION AND PERSPECTIVES

This work presents a mathematical model for the start-up flow of a drilling fluid in a horizontal pipe. The flow of a Bingham fluid, considered one-dimensional and compressible, is modeled by the conservation equations of mass and momentum. The Fanning friction factor for the Bingham fluid was employed to take into account the viscous effect. The mass and momentum conservation equations were differentiated with respect to time and space, respectively. They were subtracted from each other leading to a second order differential equation for the velocity. The resulting equation is a hyperbolic non-linear equation and is solved by an iterative numerical approach. As soon as the velocity field is known the pressure values is directly obtained from the continuity equation.

A solution for a singularity in the governing equation is proposed. Although the friction factor tends to infinity the product $f\,\mathrm{Re}^2$ goes to a constant (actually, a Hedstrom number dependent) value as the Reynolds number approaches to zero. Instead of the friction the product $f\,\mathrm{Re}^2$ is substituted into the governing equation.

The results of the current model are corroborated with the literature data for low compressibility values ($\alpha^* \leq 0.1$). For high compressibility values, the results differ from Vinay´s *et al.* (2007) data because the current model neglects the axial variations of density in the continuity equation.

A sensibility analysis with respect to Reynolds number, Bingham number and compressibility was also carried out. For low compressibility values, the pressure presents oscillations of which frequency depends on the compressibility itself (actually, on the pressure wave speed as they are related). The higher the Reynolds number the higher the pressure peaks, because of the reduction of the viscous effect. These peaks reach values five times larger than the steady state pressures. The increase of the Bingham number slightly reduces the pressure peaks but does not changes the oscillation frequency. The amplitude of the pressure peaks reduce or even vanish as the fluid compressibility increases.

## 5. ACKNOWLEDGEMENTS

The authors acknowledge the financial support from the National Agency for Petroleum, Natural Gas and Biofuels (ANP) through its Human Resources Program in UTFPR (PRH-10) and from CENPES/PETROBRAS.

## 5. REFERENCES

Chang, C.; Boger, D. V. and Nguyen, Q. D., 1998, “The Yielding of Waxy Crude Oil”, Industrial & Engineering Chemistry Research, Vol. 37, Parkville, Australia, pp. 1551-1559.

Chang, C., Rønningsen, H. P. and Nguyen, Q. D., 1999, “Isothermal Start-up of Pipeline Transporting Waxy Crude Oil”, Journal Non-Newtonian Fluid Mechanic, Vol. 87, Parkville, Australia, pp. 127-154.

Cawkwell, M. G., Charles, M. E., 1987, “An Improved Model for Start-up of Pipelines Containing Gelled Crude Oil”, Journal of Pipelines, Vol 7., pp. 41-52.

Escudier, M. P. and Presti, F, 1996, “Pipe Flow of a Thixotropic Liquid”, Journal Non-Newtonian Fluid Mechanic, Vol. 62, Liverpool, England, pp. 291-306.

Fortuna, A. O., 2000, “Técnicas Computacionais para Dinâmica dos Fluidos”, Ed. USP, 1st Edition, São Paulo, Brazil.

Rocha, L. L. V, 2007, “Start-up of Gelled Drilling Fluids, Undergraduate monograph, Mechanical Engineering Department, Federal University of Technology-UTFPR, Curitiba-PR (in Portuguese).

Sestak, J., Cawkwell, M. G., Charles, M. E. and Houskas, M., 1987, “Start-up of Gelled Crude Oil Pipelines”, Journal of Pipelines, Vol. 6, Amsterdam, Holland, pp. 15-24.

Vinay, G., Wachs, A. and Agassant, J-F., 2006, “Numerical Simulation of Weakly Compressible Bingham Flows: The Restart of Pipeline Flows of Waxy Crude Oils”, Journal of Non-Newtonian Fluid Mechanics, Vol. 136, Cedex, France, pp. 93-105.

Vinay, G., Wachs, A. and Frigaard, I., 2007, “Start-up Transients and Efficient Computation of Isothermal Waxy Crude Oil Flows”, Journal of Non-Newtonian Fluid Mechanics, Vol. 143, Cedex, France, pp. 141-156.

Wardhaugh, L. T. and Boger, D. V., 1991, “The Measurement and Description of the Yielding Behaviour of Waxy Crude Oil”, Journal of Rheology, Vol. 35 (6), pp. 1121-1156.

## 5. RESPONSIBILITY NOTICE

The authors are the only responsible for the printed material included in this paper.